Human Genomics

RESEARCH

Open Access

Epimutation analysis reveals involvement of *SLIT2/ROBO* signaling pathway in painful diabetic neuropathy

Katarzyna Malgorzata Kwiatkowska[1*†], Paolo Garagnani[1,2*†], Francesca Ferraresi[3], Massimiliano Bonafé[1,2], Maria G. Bacalini[4], Claudia Sala[1,2], Gastone Castellani[1,2], Davide Gentilini[5,6], Luciano Calzari[6], Dan Ziegler[7], Monique M. Gerrits[8], Catharina G. Faber[9], Rayaz A. Malik[10,11], Margherita Marchi[12], Erika Salvi[12], Giuseppe Lauria[12,13†] and Chiara Pirazzini[1,2†]

Abstract

Changes in gene function or expression caused by epigenetic modifications may play a role in painful diabetic neuropathy. Two independent cohorts of patients deeply phenotyped for painful diabetic neuropathy underwent whole genome DNA methylation data analysis. Burden of rare site events at the global, chromosomal and gene level; epigenetic homogeneity for regions enriched in epivariants (epilesions) and functional analysis of the genes with stochastic phenomena was undertaken. This revealed significant involvement of the *SLIT/ROBO* signaling axis-engaged in peripheral nerve regeneration after injury, among several molecular pathways, making it an attractive therapeutic target in patients with diabetic painful neuropathy.

Keywords Neuropathic pain, Diabetic neuropathy, DNA methylation, Epigenetic drift, Epivariants, Stochastic epigenetic mutations, Biological aging

†Katarzyna Malgorzata Kwiatkowska, Paolo Garagnani contributed equally and they share co-first authorship while Giuseppe Lauria and Chiara Pirazzini are contributed equally to the last authorship.

*Correspondence:
Katarzyna Malgorzata Kwiatkowska
katarzyn.kwiatkowsk2@unibo.it
Paolo Garagnani
paolo.garagnani2@unibo.it
[1]Department of Medical and Surgical Sciences (DIMEC), University of Bologna, 40126 Bologna, Italy
[2]IRCCS Azienda Ospedaliero-Universitaria di Bologna, 40138 Bologna, Italy
[3]Department of Chemistry "Giacomo Ciamician", University of Bologna, 40126 Bologna, Italy
[4]Department of Biomedical and Neuromotor Sciences (DIBINEM), University of Bologna, 40126 Bologna, Italy
[5]Department of Brain and Behavioral Sciences, University of Pavia, 27100 Pavia, Italy
[6]Bioinformatics and Statistical Genomics Unit, Istituto Auxologico Italiano IRCCS, 20095 Cusano Milanino, Italy
[7]Institute for Clinical Diabetology, German Diabetes Center, Leibniz Center for Diabetes Research at Heinrich Heine University, 40225 Düsseldorf, Germany
[8]Department of Clinical Genetics, Maastricht University Medical Centre+, 6229 HX Maastricht, The Netherlands
[9]Department of Neurology, Institute of Mental Health and Neuroscience, Maastricht University Medical Centre+, 6229 ER Maastricht, The Netherlands
[10]Institute of Cardiovascular Sciences, Manchester University NHS Foundation Trust, Manchester Academic Health Science Centre, Manchester M13 9P, UK
[11]Weill Cornell Medicine-Qatar, P.O. Box 24144, Doha, Qatar
[12]Neuroalgology Unit, Department of Clinical Neurosciences, Fondazione IRCCS Istituto Neurologico "Carlo Besta", 20133 Milan, Italy
[13]Department of Medical Biotechnology and Translational Medicine, University of Milan, Milan, Italy

Introduction

Diabetic painful neuropathy causes significant morbidity in 20–40% of patients with diabetes [44, 46], but only 30% will get a moderate degree of pain relief with currently available pharmacotherapies [6]. Beyond traditional risk factors like duration of diabetes, hyperglycemia and hyperlipidemia [44, 45], several recent studies have demonstrated alterations in histone acetylation [40, 54], long non-coding RNA [17, 61], microRNA [1, 8], circular RNA [57, 65] and DNA methylation [30, 33, 52] in painful diabetic neuropathy. Epigenetic regulation of pain-related signaling pathways, receptors and targets, through altered cytokine release, nerve excitability and ion channel function may provide a new therapeutic approach to alleviate neuropathic pain.

Aging-related phenotypes and diseases can be traced to increased DNA mutations and deterioration of DNA methylation coherent patterns (loss of homogeneity). Epivariants—stochastic epigenetic aberrations of DNA methylation as a result of the failure or random errors in the organization and/or maintenance of the methylome or alteration of nearby DNA sequences [28], are highly specific. It is estimated that only 0.5% of epivariants is recurrent in at least 5% of people [58]. Smoking [18] and environmental exposures [13] can promote accumulation of DNA methylation and increased epivariants have been already described in aging [21], cancer [19], amyotrophic lateral sclerosis [5], neurodegenerative [10], neurodevelopmental and congenital disorders [2, 20].

This study enriches the analysis and complements the findings from our previous studies linking DNA methylation to neuropathic pain in patients with T2DM [32, 33]. We have investigated if the accumulation of stochastic epigenetic events contributes to diabetic painful neuropathy.

Materials and methods

Datasets and phenotypes

We have analyzed two non-overlapping cohorts of patients with diabetic neuropathy from the German Diabetes Center in Düsseldorf (PROPGER) and University of Manchester, UK (PROPENG). All participants provided written, informed consent for all procedures. The study was approved by the Lombardy Region Ethics Committee Section of the Fondazione IRCCS Istituto Neurologico "Carlo Besta" (no. 56, 7 November 2018) and Ethics Committee of Maastricht University (NL36128.06S.11/METC 11–2-030).

Details of the cohorts and patient phenotyping have been previously described [32, 33]. Small fiber neuropathy was evaluated in skin biopsies following established guidelines [34]. According to the criteria of Treede et al. [56] Caucasian patients with T2D and neuropathic pain for > 1 year with a score of > 4/10 on the pain intensity numeric rating scale (without analgesics) were classified as having painful diabetic neuropathy (PDN) and were compared to patients with T2D scoring < 4 on the pain intensity numeric rating scale defined as painless diabetic neuropathy (PLDN). Differences between PDN/PLDN groups for age and T2DM duration were evaluated using Student's t-test.

DNA methylation assay

Whole blood samples were collected from all study participants. DNA was extracted (Puregene Blood kit; Qiagen, Hilden, Germany), bisulfite-converted (EZ-96 DNA Methylation Kit Deep-Well; Zymo Research, Irvine, CA, USA) and used in the genome-wide methylation assay (Infinium Human MethylationEPIC BeadChip; Illumina, San Diego, CA, USA). Sample randomization was ensured in all steps.

Data manipulation

DNA methylation data was preprocessed (R v4.4.3; minfi v1.52.1) following quality control, calculation of detection p-values, removal of low-quality samples (average detection p-value < 0.05) and probes (detection p-value < 0.01 in at least one of the samples), and quantile normalization. After annotation (Human GRCh37; hg19) we removed probes: i) located on sex chromosomes, ii) mapping to loci with SNPs, iii) reported previously as non-specific, cross-reactive or masked. Beta values were calculated to assess for stochastic epigenetic aberrations.

We called epivariants applying the interquartile range (IQR) approach [21–23, 51] and by selecting the PLDN group to build the reference methylation range ([Q1 − 3 × IQR; Q3 + 3 × IQR]; where IQR = Q3 − Q1 and Q1 for 25th percentile and Q3 for 75th percentile). We classified probes as: hypo-epivariants if they had methylation values below the reference population-based range, hyper-epivariants if they exceeded the maximum IQR threshold and as non-epivariants if they fitted within the range. Outlier samples with abnormal epivariant counts were detected with Hample filter (PROPGER) or boxplot (PROPENG) and excluded from the analysis.

We further refined the data exploration by analyzing epilesions – genome regions significantly enriched in epivariants, detected using computing hypergeometric distribution p-value for a genome-sliding window of size 11. We employed hypo-epilesion and hyper-epilesion names to distinguish regions enriched in hypo- and hyper-epivariants, respectively.

Data analysis

Based on epivariant counts, for each patient we calculated the following scores: TotEpiMut = log(hypo-epivariant count + hyper-epivariant count), HypoEpiMut = log(hypo-epivariant count) and

HyperEpiMut = log(hyper-epivariant count) at the global, chromosomal and gene levels. Global analysis comprised all probes spread across the epigenome. In chromosomal analysis epivariants were grouped by chromosome annotation and logarithmic scores were chromosome-wisely recalculated. Analysis on gene level was performed only for emerged significant chromosomes, grouping epivariants based on genic annotation and computing respective gene-wise scores. PDN/PLDN group differences were analyzed using a binomial generalized linear regression model including age, sex and cell counts (naive CD8 + T cells, CD4 + T cells, exhausted cytotoxic CD8 + CD28 – CD45R – (CD8pCD28nCD45RAn) T cells, natural killer cells, granulocytes, and plasma blasts) as covariates, and correlations were verified with Pearson correlation test (R package stats v4.4.3). Cell counts were estimated with Horvath's DNA methylation age calculator [29].

Differences between the PDN/PLDN groups for the number of epilesions and number of genes affected by epilesions were assessed with a Mann–Whitney test. We compared the number of epilesion carriers (patients in which at least one epilesion was detected) for PDN/PLDN using Fisher's exact test (for contingency tables with any cell with number of events < 10) or Chi-squared test (for contingency tables with all cells with the number of events ≥ 10).

We assessed epigenetic homogeneity for each sample by calculating the variance of DNA methylation and tested for significant differences between PDN/PLDN groups applying ANOVA if the computed values presented with a normal distribution and robust linear model otherwise. The differences were evaluated after adjustment for age, sex and cell counts: CD8 + and CD4 + naive cells, CD8pCD28nCD45RAn cells, natural killer cells, granulocytes, and plasma blasts. This analysis encompassed comparison of the variance on i) global level across all probes that passed quality control and filtering steps described above, and ii) local levels focalized on particular subsets (probes of class A/B/C/D, probes involved in methylation clocks, differentially variable probes, probes on chromosomes significantly enriched in epivariants).

To gain insight on the functional consequences of the epigenetic events we performed pathway enrichment analysis combining genes which emerged from PROPGER and PROPENG cohort and uploaded them to Reactome (v93), an open-source, curated and peer-reviewed database [12]. Terms with p-value from hypergeometric distribution test below 0.01 were considered as significant. The results were corrected for multiple hypothesis testing using the Benjamini–Hochberg procedure.

Results

Cohort description

Demographic characteristics of the patient groups are summarized in Table 1. The PROPGER cohort included 72 PDN and 67 PLDN patients with a higher proportion of males than females in both the PDN and PLDN groups. Two phenotypic groups were equilibrated in sample size and matched for sex, age and T2DM duration with no significant differences between PDN and PLDN. The PROPENG cohort included 27 PDN and 65 PLDN patients with 46 males vs 19 females in the PLDN group and 18 males vs 9 females in the PDN group and duration of T2DM was significantly shorter in the PLDN compared to PDN group.

PROPGER

Global analysis of the PROPGER cohort revealed that the HypoEpiMut score was significantly higher in PDN compared to PLDN group (p-value = 0.005; Supplementary Figure S1 A). There was no significant difference for Tot- and Hyper-EpiMut scores between PDN and PLDN groups (p-value = 0.057 and p-value = 0.258; Supplementary Figure S1 B and C), respectively. None of the EpiMut scores correlated with chronological age, duration of T2DM, or sex.

Analysis at the chromosomal level revealed that the number of total epivariants was higher in PDN compared to PLDN group across all autosomes (Supplementary Figure S2), with statistically significant differences between

Table 1 Main characteristics of participants from two analyzed cohorts: PROPGER and PROPENG recruited respectively at the German Diabetes Center and at the University of Manchester

	PROPGER			PROPENG		
Cohort	**PDN**	**PLDN**	**p-value[a]**	**PDN**	**PLDN**	**p-value[a]**
N	72	67		27	65	
Sex: Female (%)	15 (21%)	14 (21%)	1.000	9 (33%)	19 (29%)	0.804
Sex: Male (%)	57 (79%)	53 (79%)		18 (67%)	46 (71%)	
Age (mean, sd)	68.82 (8.99)	69.73 (9.12)	0.554	61.97 (9.11)	64.84 (8.97)	0.173
T2DM duration (mean, sd)	13.51 (10.31)	13.60 (9.22)	0.960	13.35 (9.79)	8.96 (7.02)	<u>0.041</u>

PDN for Painful Diabetic Neuropathy, *PLDN* for Painless Diabetic Neuropathy, *T2DM* for Type 2 Diabetes Mellitus

[a]The p-value of the statistical test (Student's t-test, Chi-squared test or Fisher's exact test) comparing PDN to PLDN group

Significant p-values are underlined

PDN and PLDN for chromosomes 21, 2, 18, 6, 11, 3 and 19 (in increasing p-value order) (Fig. 1A–G). We further identified that this differential signal was accumulated in 58 genes (Table 2) with several involved in peripheral nerve regeneration (*IL4I1*, *ROBO1*), neuronal excitability (*CACNA1D*, *CELF4*) and diabetes (*SIM2*, *LONP1*). There was no significant difference in the total number of epilesions or genes affected by epilesions between the PDN and PLDN groups.

An increase in hypo-epivariants was found in all autosomes except 22 (Fig. 2) in patients with PDN compared to PLDN. In depth analysis of autosomes, identified significant differences in 43 genes between PDN and PLDN (Table 2). Several partially overlapped with the above identified genes, but there were also differences in *FGF12*, *CACNA1E* and *SLIT2*. *DUSP22* had a significantly greater hypo-epilesion number in PDN compared to PLDN (Fig. 3A).

There were no statistically significant differences in hyper-epivariants between PDN and PLDN groups across autosomes (Supplementary Figure S3). However, sliding-window analysis revealed two genes, *TRIM68* and *ISOC2*, in which hyper-epilesion carriers were significantly higher in PDN compared to PLDN (Fig. 3B).

Global variance correlated significantly with age (r = 0.173, p-value = 0.041) and estimates of: naive CD8 (r = – 0.332, p-value = 0.000), NK (r = – 0.194, p-value = 0.022), CD8pCD28nCD45 (r = 0.227, p-value = 0.007) and plasma blast (r = 0.505, p-value = 0.000) cell counts, but not naive CD4 cell counts (p-value = 0.996) in the PROPGER cohort. Correlations between global variance and estimates of naive CD8 and plasma blast cell counts remained significant in the PDN and PLDN groups when analyzed separately. The correlation with CD8pCD28nCD45RAn was also significant in the PDN. All correlations ranged from poor to fair except for estimates of the plasma blast cell count in the PDN group which was moderate. There were no significant differences in methylation variance at the global and local levels between PDN and PLDN.

PROPENG

Globally, there were no differences between PDN and PLDN groups for total, hypo- and hyper-epivariants in the PROPENG cohort. There was no correlation between the EpiMut score with age, T2DM duration or sex. There were differences in total and hyper-epivariants at chromosomes 5, 22 and 9 (Supplementary Figures S4 and S5), and in hypo-epivariants at chromosomes 22, 10 and 3 (Supplementary Figure S6) with the differential signal distributed across the genome rather than being concentrated in any particular genes. The genic aggregations mapped to the protocadherin gamma cluster (*PCDHGA1*, *PCDHGA2*, *PCDHGA3*, *PCDHGA4* and *PCDHGB1*), *LOC101928885*, *ZDHHC11* and *GRAMD3* on chromosome 5, *PRRX2* and *PCA3* on chromosome 9, and *WNT7B* and *DGCR5* on chromosome 22 (Table 2). There was an accumulation of epilesions (p-value = 0.048; Supplementary Figure S7 A), particularly hyper-epilesions (p-value = 0.038; Supplementary Figure S7 B) in PDN. There was no difference in epilesion carriers between PDN and PLDN.

Global variance correlated significantly, with NK (r = – 0.537, p-value = 0.000), CD8pCD28nCD45 (r = 0.251, p-value = 0.016) and plasma blast (r = 0.618, p-value = 0.000) cell counts in the PROPENG cohort and these correlations remained significant in the PDN and PLDN group separately, except for CD8pCD28nCD45RAn which was significant only in PLDN. There was

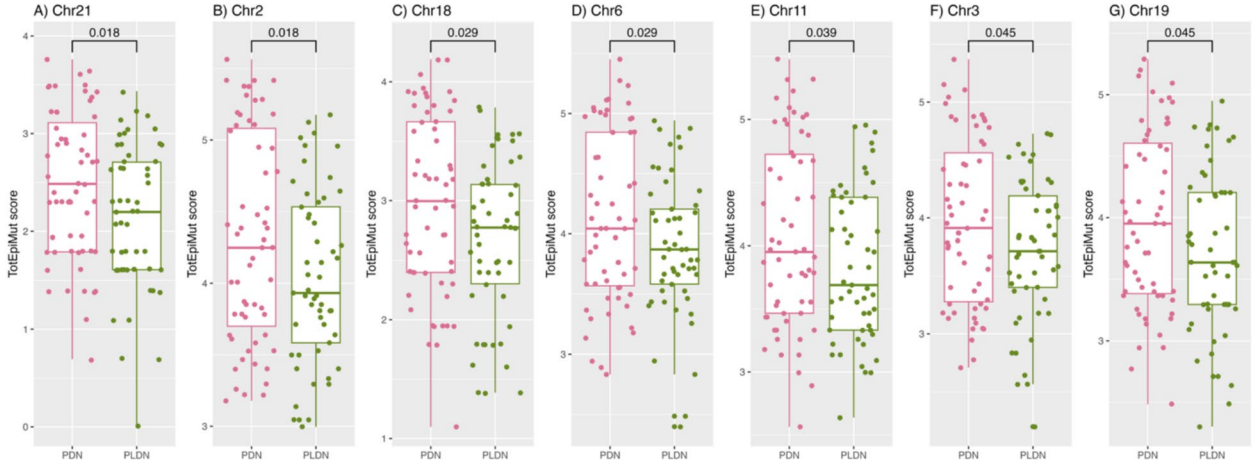

Fig. 1 Box plots of the chromosomal TotEpiMut scores which differ significantly between the PDN and PLDN groups in the PROPGER cohort. Plots visualize autosomes: **A** 21, **B** 2, **C** 18, **D** 6, **E** 11, **F** 3 and **G** 19. P-values from the binomial model with covariates age, sex and cell count estimates are indicated above the boxes

Table 2 Genes related to diabetic neuropathy pain which emerged from epivariant analysis in PROPGER and PROPENG cohorts

GeneName	SignChr	Analysis	Cohort	Avrg PLDN	Avrg PDN	p-value[a]	FDR
SIM2	chr21	TotEpiMut	PROPGER	0.132	0.407	0.031	0.996
SATB2	chr2	TotEpiMut	PROPGER	0.208	0.576	0.002	0.997
CCDC140	chr2	TotEpiMut	PROPGER	0.075	0.407	0.003	0.997
EXOC6B	chr2	TotEpiMut	PROPGER	0.057	0.254	0.004	0.997
SATB2-AS1	chr2	TotEpiMut	PROPGER	0.038	0.271	0.005	0.997
MYT1L	chr2	TotEpiMut	PROPGER	0.132	0.492	0.013	0.997
TRIP12	chr2	TotEpiMut	PROPGER	0.038	0.220	0.028	0.997
FAM178B	chr2	TotEpiMut	PROPGER	0.057	0.237	0.034	0.997
MAP2	chr2	TotEpiMut	PROPGER	0.094	0.305	0.036	0.997
LINC01280	chr2	TotEpiMut	PROPGER	0.094	0.017	0.037	0.997
GPR35	chr2	TotEpiMut	PROPGER	0.057	0.237	0.041	0.997
KLHL29	chr2	TotEpiMut	PROPGER	0.170	0.373	0.044	0.997
PAX3	chr2	TotEpiMut	PROPGER	0.075	0.254	0.044	0.997
LINC01158	chr2	TotEpiMut	PROPGER	0.038	0.237	0.046	0.997
LOC100132215	chr2	TotEpiMut	PROPGER	0.057	0.237	0.048	0.997
KCNK3	chr2	TotEpiMut	PROPGER	0.057	0.203	0.050	0.997
CELF4	chr18	TotEpiMut	PROPGER	0.302	0.814	0.001	0.395
MTCL1	chr18	TotEpiMut	PROPGER	0.038	0.169	0.047	0.992
GMDS	chr6	TotEpiMut	PROPGER	0.113	0.356	0.016	0.996
LINC00473	chr6	TotEpiMut	PROPGER	0.189	0.051	0.017	0.996
FGFR1OP	chr6	TotEpiMut	PROPGER	0.038	0.169	0.023	0.996
DUSP22	chr6	TotEpiMut	PROPGER	1.604	2.966	0.023	0.996
BTNL2	chr6	TotEpiMut	PROPGER	0.151	0.017	0.024	0.996
CDKAL1	chr6	TotEpiMut	PROPGER	0.038	0.169	0.029	0.996
SLC35D3	chr6	TotEpiMut	PROPGER	0.057	0.169	0.038	0.996
FBXO5	chr6	TotEpiMut	PROPGER	0.132	0.017	0.039	0.996
LINC00602	chr6	TotEpiMut	PROPGER	0.113	0.017	0.040	0.996
STXBP5-AS1	chr6	TotEpiMut	PROPGER	0.038	0.169	0.040	0.996
BACH2	chr6	TotEpiMut	PROPGER	0.019	0.102	0.041	0.996
USP45	chr6	TotEpiMut	PROPGER	0.113	0.017	0.042	0.996
BTN2A1	chr6	TotEpiMut	PROPGER	0.019	0.085	0.045	0.996
IL20RA	chr6	TotEpiMut	PROPGER	0.019	0.119	0.045	0.996
NEU1	chr6	TotEpiMut	PROPGER	0.094	0.017	0.046	0.996
WT1-AS	chr6	TotEpiMut	PROPGER	0.019	0.254	0.012	0.996
ABTB2	chr6	TotEpiMut	PROPGER	0.075	0.424	0.014	0.996
PAX6	chr6	TotEpiMut	PROPGER	0.264	0.678	0.021	0.996
ROBO3	chr6	TotEpiMut	PROPGER	0.075	0.288	0.026	0.996
ALX4	chr6	TotEpiMut	PROPGER	0.057	0.271	0.026	0.996
NAV2	chr6	TotEpiMut	PROPGER	0.264	0.678	0.027	0.996
IGHMBP2	chr6	TotEpiMut	PROPGER	0.019	0.169	0.028	0.996
DLG2	chr11	TotEpiMut	PROPGER	0.170	0.458	0.029	0.996
TOLLIP	chr11	TotEpiMut	PROPGER	0.075	0.271	0.029	0.996
MUC5B	chr11	TotEpiMut	PROPGER	0.019	0.169	0.043	0.996
DBX1	chr11	TotEpiMut	PROPGER	0.075	0.237	0.045	0.996
FAT3	chr11	TotEpiMut	PROPGER	0.113	0.271	0.046	0.996
ROBO1	chr11	TotEpiMut	PROPGER	0.094	0.390	0.002	0.999
PTPRG	chr11	TotEpiMut	PROPGER	0.151	0.441	0.011	0.999
LOC440982	chr11	TotEpiMut	PROPGER	0.038	0.203	0.019	0.999
ZIC4	chr11	TotEpiMut	PROPGER	0.189	0.441	0.024	0.999
CACNA1D	chr11	TotEpiMut	PROPGER	0.113	0.305	0.027	0.999
ZBTB38	chr3	TotEpiMut	PROPGER	0.094	0.288	0.035	0.999
FGF12	chr3	TotEpiMut	PROPGER	0.094	0.356	0.037	0.999

Table 2 (continued)

GeneName	SignChr	Analysis	Cohort	Avrg PLDN	Avrg PDN	p-value[a]	FDR
TMEM108	chr3	TotEpiMut	PROPGER	0.038	0.119	0.049	0.999
CHL1	chr3	TotEpiMut	PROPGER	0.038	0.136	0.050	0.999
IL4I1	chr19	TotEpiMut	PROPGER	0.019	0.136	0.038	0.998
LONP1	chr19	TotEpiMut	PROPGER	0.038	0.220	0.042	0.998
SPTBN4	chr19	TotEpiMut	PROPGER	0.075	0.203	0.047	0.998
CHST8	chr19	TotEpiMut	PROPGER	0.170	0.424	0.049	0.998
VWA5B1	chr1	HypoEpiMut	PROPGER	0.020	0.179	0.029	0.993
AJAP1	chr1	HypoEpiMut	PROPGER	0.041	0.196	0.043	0.993
CACNA1E	chr1	HypoEpiMut	PROPGER	0.061	0.214	0.050	0.993
MYT1L	chr2	HypoEpiMut	PROPGER	0.061	0.375	0.010	0.992
LINC01237	chr2	HypoEpiMut	PROPGER	0.122	0.393	0.027	0.992
STON1-GTF2A1L	chr2	HypoEpiMut	PROPGER	0.020	0.286	0.034	0.992
ROBO1	chr3	HypoEpiMut	PROPGER	0.020	0.304	0.009	0.992
FGF12	chr3	HypoEpiMut	PROPGER	0.041	0.214	0.029	0.992
AFAP1	chr4	HypoEpiMut	PROPGER	0.082	0.375	0.004	0.992
FAT1	chr4	HypoEpiMut	PROPGER	0.061	0.268	0.035	0.992
SLIT2	chr4	HypoEpiMut	PROPGER	0.041	0.179	0.037	0.992
DCHS2	chr4	HypoEpiMut	PROPGER	0.143	0.018	0.042	0.992
ERGIC1	chr5	HypoEpiMut	PROPGER	0.082	0.375	0.022	0.992
AHRR	chr5	HypoEpiMut	PROPGER	0.020	0.196	0.047	0.992
RNF130	chr5	HypoEpiMut	PROPGER	0.061	0.214	0.050	0.992
GMDS	chr6	HypoEpiMut	PROPGER	0.061	0.250	0.019	0.992
DUSP22	chr6	HypoEpiMut	PROPGER	1.571	2.964	0.046	0.992
PTN	chr7	HypoEpiMut	PROPGER	0.041	0.196	0.026	0.994
LINC00535	chr8	HypoEpiMut	PROPGER	0.020	0.196	0.034	0.992
ST18	chr8	HypoEpiMut	PROPGER	0.061	0.214	0.041	0.992
PAPPA	chr9	HypoEpiMut	PROPGER	0.020	0.196	0.044	0.992
RXRA	chr9	HypoEpiMut	PROPGER	0.041	0.179	0.045	0.992
GRID1	chr10	HypoEpiMut	PROPGER	0.082	0.339	0.018	0.994
NAV2	chr11	HypoEpiMut	PROPGER	0.102	0.393	0.027	0.992
DLG2	chr11	HypoEpiMut	PROPGER	0.082	0.286	0.040	0.992
LOC101928989	chr11	HypoEpiMut	PROPGER	0.020	0.143	0.047	0.992
ANKS1B	chr12	HypoEpiMut	PROPGER	0.020	0.250	0.018	0.992
GALNT9	chr12	HypoEpiMut	PROPGER	0.224	0.589	0.034	0.992
OCA2	chr15	HypoEpiMut	PROPGER	0.122	0.393	0.013	0.992
AGBL1	chr15	HypoEpiMut	PROPGER	0.061	0.286	0.024	0.992
NR2F2-AS1	chr15	HypoEpiMut	PROPGER	0.041	0.196	0.046	0.992
ATP2C2	chr16	HypoEpiMut	PROPGER	0.041	0.250	0.020	0.992
CASC16	chr16	HypoEpiMut	PROPGER	0.020	0.161	0.033	0.992
GSG1L	chr16	HypoEpiMut	PROPGER	0.041	0.196	0.039	0.992
CLCN7	chr16	HypoEpiMut	PROPGER	0.224	0.607	0.041	0.992
CHST4	chr16	HypoEpiMut	PROPGER	0.041	0.179	0.044	0.992
NXN	chr17	HypoEpiMut	PROPGER	0.122	0.429	0.037	0.993
CA10	chr17	HypoEpiMut	PROPGER	0.020	0.179	0.040	0.993
CELF4	chr18	HypoEpiMut	PROPGER	0.061	0.232	0.031	0.996
ZBTB45	chr19	HypoEpiMut	PROPGER	0.061	0.214	0.036	0.992
MYO1F	chr19	HypoEpiMut	PROPGER	0.041	0.214	0.044	0.992
LOC63930	chr20	HypoEpiMut	PROPGER	0.020	0.196	0.025	0.992
ISM1	chr20	HypoEpiMut	PROPGER	0.020	0.143	0.052	0.992
WNT7B	chr22	TotEpiMut	PROPENG	0.362	0.043	0.026	0.995
DGCR5	chr22	TotEpiMut	PROPENG	0.034	0.217	0.038	0.995
PCDHGA1	chr5	TotEpiMut	PROPENG	1.328	0.174	0.005	0.997

Table 2 (continued)

GeneName	SignChr	Analysis	Cohort	Avrg PLDN	Avrg PDN	p-value[a]	FDR
PCDHGA2	chr5	TotEpiMut	PROPENG	1.259	0.174	0.007	0.997
PCDHGA3	chr5	TotEpiMut	PROPENG	1.155	0.174	0.013	0.997
PCDHGB1	chr5	TotEpiMut	PROPENG	1.069	0.174	0.026	0.997
LOC101928885	chr5	TotEpiMut	PROPENG	0.017	0.043	0.047	0.997
ZDHHC11	chr5	TotEpiMut	PROPENG	0.017	0.087	0.049	0.997
PRRX2	chr9	TotEpiMut	PROPENG	0.017	0.130	0.036	0.998
PCA3	chr9	TotEpiMut	PROPENG	0.017	0.043	0.047	0.998
PCDHGA1	chr5	HyperEpiMut	PROPENG	1.241	0.130	0.014	0.996
PCDHGA2	chr5	HyperEpiMut	PROPENG	1.155	0.130	0.018	0.996
PCDHGA3	chr5	HyperEpiMut	PROPENG	1.069	0.130	0.021	0.996
PCDHGB1	chr5	HyperEpiMut	PROPENG	0.983	0.130	0.028	0.996
GRAMD3	chr5	HyperEpiMut	PROPENG	0.052	0.217	0.030	0.996
PCDHGA4	chr5	HyperEpiMut	PROPENG	0.862	0.130	0.040	0.996
DGCR5	chr22	HyperEpiMut	PROPENG	0.017	0.174	0.043	0.998

SignChr for Significant Chromosome, *AvrgPLDN/AvrgPDN* for mean number of epivariants in PLDN/PDN group; FDR for False Discovery Rate calculated with Benjamini–Hochberg method

[a]The p-value of the statistical test (binomial generalized linear regression model including age, sex and cell counts) comparing PDN to PLDN group

Significant p-values are underlined

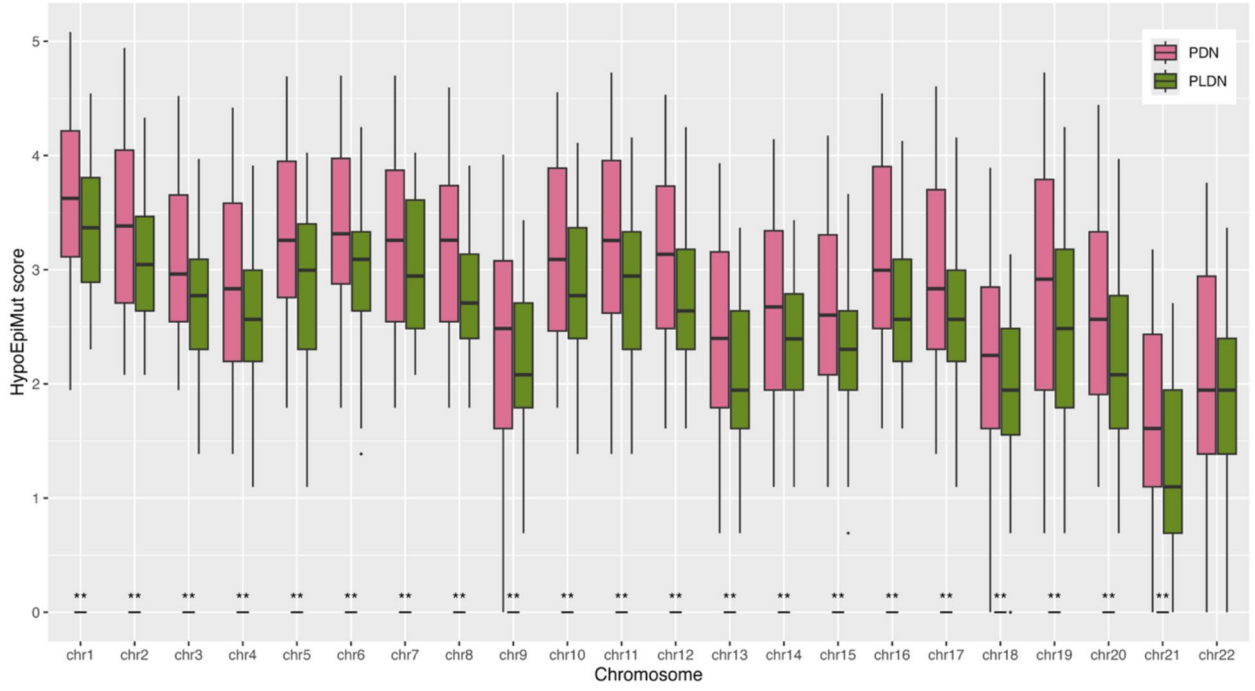

Fig. 2 Visualization of chromosomal HypoEpiMut scores in the PROPGER PDN and PLDN groups across all autosomes. Significant differences are marked with asterisks: * p-value < 0.05, ** adjusted p-value < 0.05

no significant difference in methylation variance at the global and local levels between PDN and PLDN.

Functional analysis

Pathway enrichment analysis of 107 unique identified genes (105 from epivariant and 2 from epilesion analysis), revealed nine relevant pathways listed in Table 3. "Regulation of commissural axon pathfinding by *SLIT* and *ROBO*" (R-HSA-428542) survived Benjamini–Hochberg correction. Five other pathways including "Regulation of expression of *SLIT*s and *ROBO*s" (R-HSA-9010553), "*SLIT2:ROBO1* increases *RHOA* activity" (R-HSA-8985586), "Role of *ABL* in *ROBO-SLIT* signaling" (R-HSA-428890), "Inactivation of *CDC42* and *RAC1*" (R-HSA-428543) and "Activation of *RAC1*" (R-HSA-428540) are related to the *SLIT*/*ROBO* axis and

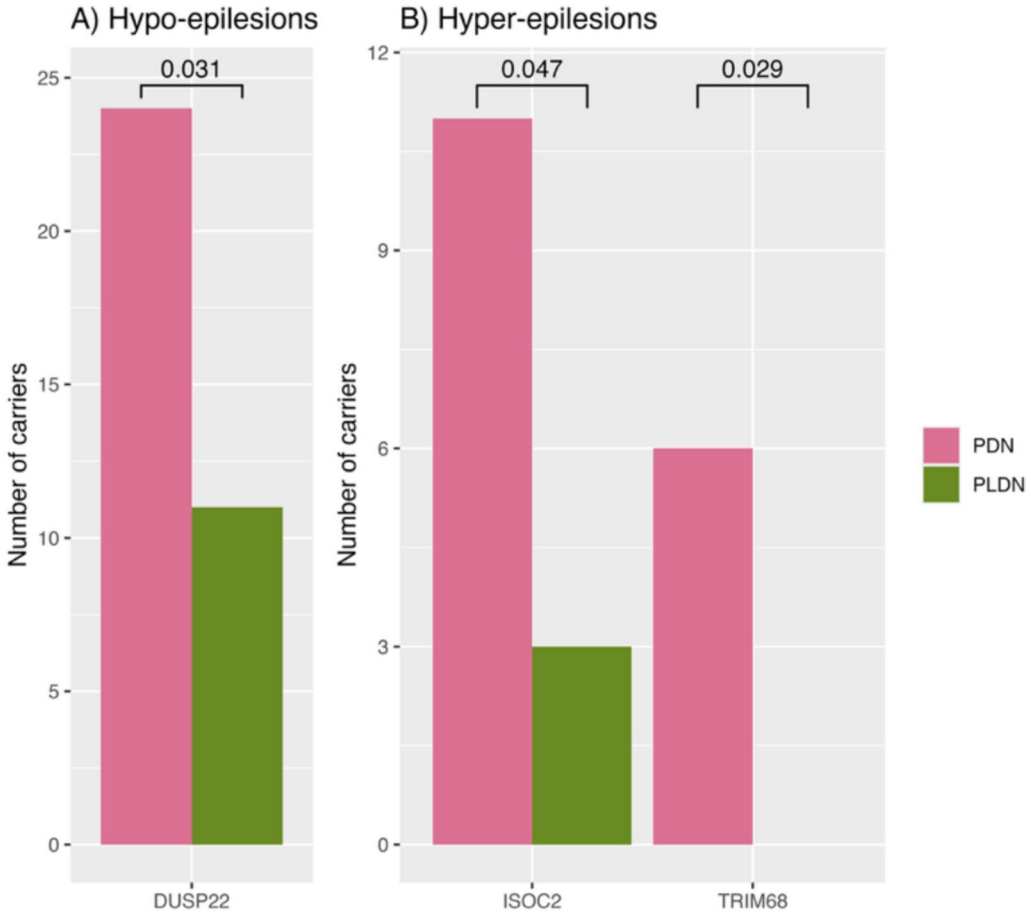

Fig. 3 Summary of outcome of epilesion analysis in the PROPGER cohort. Bar plots present number of **A** hypo-epilesion and **B** hyper-epilesion carriers in genes which differed significantly between PDN and PLDN groups

Table 3 Results of pathway enrichment analysis against Reactome database

Pathway name	N genes found/total	Gene ratio	p-value[a]	FDR	N reactions[b] found/total	Reactions ratio
Regulation of commissural axon pathfinding by *SLIT* and *ROBO*	3/12	0.001	0.000	0.024	5/5	0.000
Regulation of expression of *SLIT*s and *ROBO*s	6/170	0.011	0.001	0.128	13/20	0.001
SLIT2:*ROBO1* increases *RHOA* activity	2/8	0.000	0.002	0.128	2/2	0.000
Role of *ABL* in *ROBO*-*SLIT* signaling	2/10	0.001	0.002	0.139	4/4	0.000
Inactivation of *CDC42* and *RAC1*	2/12	0.001	0.003	0.139	4/4	0.000
Butyrophilin (*BTN*) family interactions	2/12	0.001	0.003	0.139	2/8	0.001
Signaling by *ROBO* receptors	6/222	0.014	0.005	0.162	49/60	0.004
Activation of *RAC1*	2/15	0.001	0.005	0.162	4/4	0.000
Formation of the anterior neural plate	2/19	0.001	0.008	0.223	2/15	0.001

N for Number, *FDR* for False Discovery Rate calculated with Benjamini–Hochberg method

[a]The p-value of the statistical test (hypergeometric distribution test) determining whether particular Reactome pathways are over-represented (enriched) in the submitted data

[b]Reaction corresponds to any event in biology that changes the state of a biological molecule

Significant p-values are underlined

all belong to the same "Signaling by *ROBO* receptors" (R-HSA-376176) parent term. Two additional significant pathways were "Butyrophilin (*BTN*) family interactions" (R-HSA-8851680) and "Formation of the anterior neural plate" (R-HSA-9823739) and correspond to adaptive immune system and neurodevelopmental mechanisms, respectively.

Discussion

We recently demonstrated alterations in differential DNA methylation [33] and DNAm age acceleration [32] in patients with painful diabetic neuropathy. In the same two cohorts we now identify epigenetic alterations characterized by changes in total burden, chromosomal distribution, genic accumulation, and aberration-enriched regions without loss of DNA methylation homogeneity in patients with painful compared to painless diabetic neuropathy. Functional analysis revealed an important role of the multilayer *SLIT-ROBO* axis and its regulation with particular involvement of *SLIT2*, *ROBO1*, *ROBO3* genes that were enriched in epivariants in patients with painful diabetic neuropathy. Further analysis of stochastic epigenetic aberrations of DNA methylation revealed differences in *FGF12*, *CACNA1D*, *CACNA1E*, gamma protocadherins (*PCDHGA1*, *PCDHGA2*, *PCDHGA3*, *PCDHGA4*, *PCDHGB1*), *TFAP2A* and *IL4I1* genes.

SLIT2 is a member of highly conserved family of glycoproteins regulating neuronal axon guidance, cell proliferation, cell migration and vascularisation [55]. In pathologies of central nervous system, *SLIT*/*ROBO* signaling influences neuronal migration, axonal projection, chemorepulsion, leukocyte migration, neuroinflammation, angiogenesis and blood brain barrier permeability/stability [50]. mRNA profiling in mouse models of chronic pain, in particular inflammatory and neuropathic pain, have revealed dysregulation of both, *SLIT2* and *ROBO1* genes [9, 31]. Involvement of *SLIT2*/*ROBO1* in peripheral nerve regeneration and functional recovery after injury [36, 50, 53], among several molecular pathways, make this axis a potential therapeutic target for peripheral nerve injuries, and neuropathic pain [50].

FGF12 is a key modulator of voltage-gated sodium channels [4] affecting the voltage dependence and rapid inactivation of Nav1.2 and Nav1.6 channels [49], and also induces resurgent currents produced by Nav1.8 and Nav1.9 [60]. Altered function of several sodium channels has been implicated in acute and persistent pain signaling [3] and genetic alterations in $Na_v1.3$, $Na_v1.7$, $Na_v1.8$, $Na_v1.9$ are associated with changes in neuron excitability and nociceptive thresholds linked to neuropathic pain [16, 25, 37, 43, 48]. Therapeutic molecules (toxins, antibodies, small molecules etc.) targeting these voltage-gated sodium channels are being developed for painful neuropathy.

CACNA1D and *CACNA1E* encode $Ca_v1.3$ and $Ca_v2.3$ subunits of calcium high-voltage activated channels, respectively. $Ca_v1.3$ in particular regulates physiological functions in cochlear inner hair, sinoatrial node, and neurons [63]. To date, 80 de novo missense variants of *CACNA1D* have been associated with diseases including autism spectrum disorder, hyperactivity, muscle hypotonia, intellectual impairment, developmental delay and seizures [41, 42]. $Ca_v2.3$ is expressed predominantly in the brain and is involved in neurotransmitter release and synaptic plasticity [59] and carriers of *CACNA1E* mutations manifest with encephalopathy, macrocephaly, dyskinesias, and epilepsy [7, 27]. Several *CACNA1D* and *CACNA1E* SNPs have also been linked to T2DM [15].

The PROPENG cohort has additionally revealed alterations in protocadherin gamma cluster genes (*PCDHG@*) which encode cell-surface homophilic proteins [24], regulate nervous system development and dendritic self-avoidance, dendrite arborization, neuronal survival, astrocyte-neuron interactions, and axonal tiling [11, 26, 35]. Furthermore, Metltzer et al. [39] described distinct functions of specific *PCDHG@* isoforms in relation to central mechanosensory circuitry assembly, essential for behavioral reactivity to touch. Additionally, a recent study has shown that *PCDHG@* may play an important role in regeneration of adult sensory neurons and skin rewiring [38]. In a sciatic nerve injury model a significant association has been reported between *TFAP2A* expression levels and the proliferation and migration of Schwann cells, which are key to functional recovery of injured nerves [64]. Furthermore, *TFAP2A* has been shown to modulate neuropathic pain through positive regulation of *GRIN1* – the gene mediating expression of pro-inflammatory factors which enhance neuronal excitability and increase hypersensitivity [62]. Interleukin 4 Induced gene 1 (*IL4I1*) has been shown to be involved in remyelination [47] through regulation of T cell expansion and modulation of inflammation. There is also evidence that the Interleukin 4 gene, is involved in nerve repair and neuropathic pain [14], but the functional link between *IL4I1* and *IL4* remains unclear. Epivariant analysis also revealed alterations in *MYT1L*, *EXOC6B*, *PAX6*, and *RNF130* genes which have previously been shown to be differentially methylated in PDN and PLDN [33], confirming multidimensional epigenetic involvement of these genes in painful diabetic neuropathy.

To conclude, these findings reinforce the evidence for involvement of DNA methylation in the regulation of neuropathic pain in diabetes. The identification of epigenetic modifications further develops our understanding of the complex underlying mechanisms and development of novel therapeutic approaches for the currently inadequate treatment of painful diabetic neuropathy.

Supplementary Information

The online version contains supplementary material available at https://doi.org/10.1186/s40246-025-00905-8.

Supplementary Material 1.

Acknowledgements
The authors thank the Ministry of University and Research (MUR), NextGenerationEU, National Recovery and Resilience Plan, project MNESYS (PE0000006): "A Multiscale integrated approach to the study of the nervous system in health and disease" (DN.1553 11.10.2022).

Author contributions
Conceptualization: PG, KMK, CP, GL, CGF. Data curation: KMK, PG, CP. Formal analysis: KMK, FF. Statistical analysis: KMK, CS. Funding acquisition: GL, PG. Investigation: KMK, PG, CP. Methodology: KMK, CP, MGB, DG, LC. Resources: PG, CP, GL, DZ, MMG, CGF, MB, GC. Supervision: PG, GL. Visualization: KMK, MM, ES. Writing—original draft: KMK, PG. Writing—review and editing: KMK, PG, GL, CP, RAM. All authors have read and approved submitted manuscript.

Funding
This work was supported by the European Union's Horizon 2020 research and innovation programme under the Marie Skłodowska-Curie Grant Agreement No. 721841 PainNET and the Italian Ministry of Health (RRC).

Data availability
The datasets generated and analyzed during the current study are available in the GEO NCBI repository under accession number GSE286347.

Declarations

Ethics approval
This study has been performed in accordance with the Declaration of Helsinki. The study was approved by the Lombardy Region Ethics Committee Section of the Fondazione IRCCS Istituto Neurologico "Carlo Besta" (no. 56, 7 November 2018) and Ethics Committee of Maastricht University (NL36128.06S.11/METC 11-2-030).

Consent to participate
All participants provided written, informed consent for participation in the study.

Competing interests
The authors declare no competing interests.

Received: 17 November 2025 / Accepted: 24 December 2025
Published online: 09 January 2026

References

1. Amir Mahmoudi Aghdam, Parviz Shahabi, Elham Karimi-Sales, Rafigheh Ghiasi, Saeed Sadigh-Eteghad, Javad Mahmoudi, Mohammad Reza Alipour. Swimming Exercise Induced Reversed Expression of miR-96 and Its Target Gene NaV1.3 in Diabetic Peripheral Neuropathy in Rats. Chin J Physiol 2018;61.
2. Barbosa M, Joshi RS, Garg P, Martin-Trujillo A, Patel N, Jadhav B, et al. Identification of rare de novo epigenetic variations in congenital disorders. Nat Commun. 2018;9:2064.
3. Bennett DL, Clark AJ, Huang J, Waxman SG, Dib-Hajj SD. The role of voltage-gated sodium channels in pain signaling. Physiol Rev. 2019;99:1079–151.
4. Biadun M, Karelus R, Krowarsch D, Opalinski L, Zakrzewska M. FGF12: biology and function. Differentiation. 2024;139:100740.
5. Brusati A, Peverelli S, Calzari L, Tiloca C, Casiraghi V, Sorce MN, et al. Exploring epigenetic drift and rare epivariations in amyotrophic lateral sclerosis by epigenome-wide association study. Front Aging Neurosci. 2023;15:1272135.
6. Callaghan BC, Cheng HT, Stables CL, Smith AL, Feldman EL. Diabetic neuropathy: clinical manifestations and current treatments. Lancet Neurol. 2012;11:521–34.
7. Carvill GL. Calcium channel dysfunction in epilepsy: gain of CACNA1E. Epilepsy Curr. 2019;19:199–201.
8. Chattopadhyay M, Zhou Z, Hao S, Mata M, Fink DJ. Reduction of Voltage Gated Sodium Channel Protein in DRG by Vector Mediated miRNA Reduces Pain in Rats with Painful Diabetic Neuropathy. Mol Pain 2012;8:1744-8069-8–17.
9. Chen B, Carr L, Dun X-P. Dynamic expression of Slit1–3 and Robo1–2 in the mouse peripheral nervous system after injury. Neural Regen Res. 2020;15:948.
10. Chen GK, Yan Q, Paul KC, Kusters CDJ, Folle AD, Furlong M, et al. Stochastic epigenetic mutations influence Parkinson's disease risk, progression, and mortality. J Parkinsons Dis. 2022;12:545–56.
11. Chen WV, Alvarez FJ, Lefebvre JL, Friedman B, Nwakeze C, Geiman E, et al. Functional significance of isoform diversification in the protocadherin gamma gene cluster. Neuron. 2012;75:402–9.
12. Croft D, O'Kelly G, Wu G, Haw R, Gillespie M, Matthews L, et al. Reactome: a database of reactions, pathways and biological processes. Nucleic Acids Res. 2011;39:D691-697.
13. Curtis SW, Kilaru V, Terrell ML, Marder ME, Barr DB, Marsit CJ, et al. Exposure to polybrominated biphenyl and stochastic epigenetic mutations: application of a novel epigenetic approach to environmental exposure in the Michigan polybrominated biphenyl registry. Epigenetics. 2019;14:1003–18.
14. Daines JM, Schellhardt L, Wood MD. The role of the IL-4 signaling pathway in traumatic nerve injuries. Neurorehabil Neural Repair. 2021;35:431–43.
15. Díaz-García JD, Leyva-Leyva M, Sánchez-Aguillón F, de León-Bautista MP, Fuentes-Venegas A, Torres-Viloria A, et al. Association study of CACNA1D, KCNJ11, KCNQ1, and CACNA1E single-nucleotide polymorphisms with type 2 diabetes mellitus. Int J Mol Sci. 2024;25:9196.
16. Dib-Hajj SD, Black JA, Waxman SG. NaV1.9: a sodium channel linked to human pain. Nat Rev Neurosci. 2015;16:511–9.
17. Du H, Liu Z, Tan X, Ma Y, Gong Q. Identification of the genome-wide expression patterns of long non-coding RNAs and mRNAs in mice with streptozotocin-induced diabetic neuropathic pain. Neuroscience. 2019;402:90–103.
18. Fiorito G, McCrory C, Robinson O, Carmeli C, Ochoa-Rosales C, Zhang Y, Colicino E, Dugué P-A, Artaud F, McKay GJ, Jeong A, Mishra PP, Nøst TH, Krogh V, Panico S, Sacerdote C, Tumino R, Palli D, Matullo G, Guarrera S, Gandini M, Bochud M, Dermitzakis E, Muka T, Schwartz J, Vokonas PS, Just A, Hodge AM, Giles GG, Southey MC, Hurme MA, Young I, McKnight AJ, Kunze S, Waldenberger M, Peters A, Schwettmann L, Lund E, Baccarelli A, Milne RL, Kenny RA, Elbaz A, Brenner H, Kee F, Voortman T, Probst-Hensch N, Lehtimäki T, Elliot P, Stringhini S, Vineis P, Polidoro S, BIOS Consortium, Lifepath consortium. Socioeconomic position, lifestyle habits and biomarkers of epigenetic aging: a multi-cohort analysis. Aging (Albany NY) 2019;11:2045–2070.
19. Gagliardi A, Dugué P-A, Nøst TH, Southey MC, Buchanan DD, Schmidt DF, et al. Stochastic epigenetic mutations are associated with risk of breast cancer, lung cancer, and mature B-cell neoplasms. Cancer Epidemiol Biomarkers Prev. 2020;29:2026–37.
20. Garg P, Sharp AJ. Screening for rare epigenetic variations in autism and schizophrenia. Hum Mutat. 2019;40:952–61.
21. Gentilini D, Garagnani P, Pisoni S, Bacalini MG, Calzari L, Mari D, et al. Stochastic epigenetic mutations (DNA methylation) increase exponentially in human aging and correlate with X chromosome inactivation skewing in females. Aging. 2015;7:568–78.
22. Gentilini D, Scala S, Gaudenzi G, Garagnani P, Capri M, Cescon M, et al. Epigenome-wide association study in hepatocellular carcinoma: identification of stochastic epigenetic mutations through an innovative statistical approach. Oncotarget. 2017;8:41890–902.
23. Gentilini D, Somigliana E, Pagliardini L, Rabellotti E, Garagnani P, Bernardinelli L, et al. Multifactorial analysis of the stochastic epigenetic variability in cord blood confirmed an impact of common behavioral and environmental factors but not of in vitro conception. Clin Epigenetics. 2018;10:77.
24. Goodman KM, Rubinstein R, Thu CA, Mannepalli S, Bahna F, Ahlsén G, et al. γ-Protocadherin structural diversity and functional implications. Elife. 2016;5:e20930.
25. Hameed S. Nav1.7 and Nav1.8: role in the pathophysiology of pain. Mol Pain. 2019;15:1744806919858801.
26. Hasegawa S, Kumagai M, Hagihara M, Nishimaru H, Hirano K, Kaneko R, et al. Distinct and Cooperative Functions for the Protocadherin-α, -β and -γ Clusters in Neuronal Survival and Axon Targeting. Front Mol Neurosci. 2016. https://doi.org/10.3389/fnmol.2016.00155.
27. Helbig KL, Lauerer RJ, Bahr JC, Souza IA, Myers CT, Uysal B, Schwarz N, Gandini MA, Huang S, Keren B, Mignot C, Afenjar A, Billette De Villemeur T, Héron D, Nava C, Valence S, Buratti J, Fagerberg CR, Soerensen KP, Kibaek M, Kamsteeg

E-J, Koolen DA, Gunning B, Schelhaas HJ, Kruer MC, Fox J, Bakhtiari S, Jarrar R, Padilla-Lopez S, Lindstrom K, Jin SC, Zeng X, Bilguvar K, Papavasileiou A, Xing Q, Zhu C, Boysen K, Vairo F, Lanpher BC, Klee EW, Tillema J-M, Payne ET, Cousin MA, Kruisselbrink TM, Wick MJ, Baker J, Haan E, Smith N, Sadeghpour A, Davis EE, Katsanis N, Corbett MA, MacLennan AH, Gecz J, Biskup S, Goldmann E, Rodan LH, Kichula E, Segal E, Jackson KE, Asamoah A, Dimmock D, McCarrier J, Botto LD, Filloux F, Tvrdik T, Cascino GD, Klingerman S, Neumann C, Wang R, Jacobsen JC, Nolan MA, Snell RG, Lehnert K, Sadleir LG, Anderlid B-M, Kvarnung M, Guerrini R, Friez MJ, Lyons MJ, Leonhard J, Kringlen G, Casas K, El Achkar CM, Smith LA, Rotenberg A, Poduri A, Sanchis-Juan A, Carss KJ, Rankin J, Zeman A, Raymond FL, Blyth M, Kerr B, Ruiz K, Urquhart J, Hughes I, Banka S, Hedrich UBS, Scheffer IE, Helbig I, Zamponi GW, Lerche H, Mefford HC, Allori A, Angrist M, Ashley P, Bidegain M, Boyd B, Chambers E, Cope H, Cotten CM, Curington T, Davis EE, Ellestad S, Fisher K, French A, Gallentine W, Goldberg R, Hill K, Kansagra S, Katsanis N, Katsanis S, Kurtzberg J, Marcus J, McDonald M, Mikati M, Miller S, Murtha A, Perilla Y, Pizoli C, Purves T, Ross S, Sadeghpour A, Smith E, Wiener J. De Novo Pathogenic Variants in CACNA1E Cause Developmental and Epileptic Encephalopathy with Contractures, Macrocephaly, and Dyskinesias. The American Journal of Human Genetics 2018;103:666–678.

28. Horsthemke B. Epimutations in Human Disease. In: Doerfler W, Böhm P, editors. DNA methylation: development, genetic disease and cancer. Current Topics in Microbiology and Immunology. Springer Berlin Heidelberg, 2006, Vol. 310. pp. 45–59. https://doi.org/10.1007/3-540-31181-5_4.
29. Horvath S. Erratum to: DNA methylation age of human tissues and cell types. Genome Biol. 2015;16:96.
30. Jang J-H, Song E-M, Do Y-H, Ahn S, Oh J-Y, Hwang T-Y, et al. Acupuncture alleviates chronic pain and comorbid conditions in a mouse model of neuropathic pain: the involvement of DNA methylation in the prefrontal cortex. Pain. 2021;162:514–30.
31. Ke C, Gao F, Tian X, Li C, Shi D, He W, et al. Slit2/Robo1 mediation of synaptic plasticity contributes to bone cancer pain. Mol Neurobiol. 2017;54:295–307.
32. Kwiatkowska KM, Garagnani P, Bonafé M, Bacalini MG, Calzari L, Gentilini D, et al. Painful diabetic neuropathy is associated with accelerated epigenetic aging. Geroscience. 2025;47:4041–54.
33. Kwiatkowska KM, Garagnani P, Bonafé M, Bacalini MG, Sala C, Castellani G, et al. High-resolution whole-genome DNA methylation revealed unique signatures of painful diabetic neuropathy. Diabetes. 2025;74:640–50.
34. Lauria G, Cornblath DR, Johansson O, McArthur JC, Mellgren SI, Nolano M, Rosenberg N, Sommer C, European Federation of Neurological Societies. EFNS guidelines on the use of skin biopsy in the diagnosis of peripheral neuropathy. Eur J Neurol 2005;12:747–758.
35. Lefebvre JL, Kostadinov D, Chen WV, Maniatis T, Sanes JR. Protocadherins mediate dendritic self-avoidance in the mammalian nervous system. Nature. 2012;488:517–21.
36. Li Y, Gao Y, Xu X, Shi R, Liu J, Yao W, et al. Slit2/Robo1 promotes synaptogenesis and functional recovery of spinal cord injury. NeuroReport. 2017;28:75–81.
37. Liao S, Liu T, Yang R, Tan W, Gu J, Deng M. Structure and function of sodium channel Nav1.3 in neurological disorders. Cell Mol Neurobiol. 2023;43:575–84.
38. Long RM, Ong H, Wang WX, Komirishetty P, Areti A, Chandrasekhar A, et al. The role of protocadherin γ in adult sensory neurons and skin reinnervation. J Neurosci. 2023;43:8348–66.
39. Meltzer S, Boulanger KC, Chirila AM, Osei-Asante E, DeLisle M, Zhang Q, et al. γ-Protocadherins control synapse formation and peripheral branching of touch sensory neurons. Neuron. 2023;111:1776-1794.e10.
40. Michelson D, Chin WW, Dworkin RH, Freeman R, Herrmann DN, Mazitschek R, Pop-Busui R, Shaibani A, Vornov J, Jones M, Jarpe M, Hader B, Viera T, Hylan M, Kachmar T, Jones S. A randomized, double-blind, placebo-controlled study of histone deacetylase type 6 inhibition for the treatment of painful diabetic peripheral neuropathy. PR9 2023;8:e1114.
41. Ortner NJ. CACNA1D-Related Channelopathies: From Hypertension to Autism. In: Striessnig J, editor. Voltage-gated Ca2+ Channels: Pharmacology, Modulation and their Role in Human Disease. Handbook of Experimental Pharmacology. Cham: Springer International Publishing, 2023, Vol. 279. pp. 183–225. https://doi.org/10.1007/164_2022_626.
42. Ortner NJ, Kaserer T, Copeland JN, Striessnig J. De novo CACAN1D Ca2+ channelopathies: clinical phenotypes and molecular mechanism. Pflugers Arch Eur J Physiol. 2020;472:755–73.
43. Osteen JD, Herzig V, Gilchrist J, Emrick JJ, Zhang C, Wang X, et al. Selective spider toxins reveal a role for the Nav11 channel in mechanical pain. Nature. 2016;534:494–9.
44. Ponirakis G, Elhadd T, Al Ozairi E, Brema I, Chinnaiyan S, Taghadom E, et al. Prevalence and risk factors for diabetic peripheral neuropathy, neuropathic pain and foot ulceration in the Arabian Gulf region. J Diabetes Investig. 2022;13:1551–9.
45. Ponirakis G, Elhadd T, Chinnaiyan S, Hamza AH, Sheik S, Kalathingal MA, et al. Prevalence and risk factors for diabetic neuropathy and painful diabetic neuropathy in primary and secondary healthcare in Qatar. J Diabetes Investig. 2021;12:592–600.
46. Pop-Busui R, Boulton AJM, Feldman EL, Bril V, Freeman R, Malik RA, et al. Diabetic neuropathy: a position statement by the American Diabetes Association. Diabetes Care. 2017;40:136–54.
47. Psachoulia K, Chamberlain KA, Heo D, Davis SE, Paskus JD, Nanescu SE, et al. IL4I1 augments CNS remyelination and axonal protection by modulating T cell driven inflammation. Brain. 2016;139:3121–36.
48. Ren Y-S, Qian N-S, Tang Y, Liao Y-H, Yang Y-L, Dou K-F, et al. Sodium channel Nav1.6 is up-regulated in the dorsal root ganglia in a mouse model of type 2 diabetes. Brain Res Bull. 2012;87:244–9.
49. Seiffert S, Pendziwiat M, Bierhals T, Goel H, Schwarz N, van der Ven A, et al. Modulating effects of FGF12 variants on NaV1.2 and NaV1.6 being associated with developmental and epileptic encephalopathy and Autism spectrum disorder: a case series. EBioMedicine. 2022;83:104234.
50. Sherchan P, Travis ZD, Tang J, Zhang JH. The potential of Slit2 as a therapeutic target for central nervous system disorders. Expert Opin Ther Targets. 2020;24:805–18.
51. Spada E, Calzari L, Corsaro L, Fazia T, Mencarelli M, Di Blasio AM, et al. Epigenome wide association and stochastic epigenetic mutation analysis on cord blood of preterm birth. Int J Mol Sci. 2020;21:5044.
52. Sun L, Gu X, Pan Z, Guo X, Liu J, Atianjoh FE, et al. Contribution of DNMT1 to neuropathic pain genesis partially through epigenetically repressing *Kcna2* in primary afferent neurons. J Neurosci. 2019;39:6595–607.
53. Tanno T, Fujiwara A, Takenaka S, Kuwamura M, Tsuyama S. Expression of a chemorepellent factor, Slit2, in peripheral nerve regeneration. Biosci Biotechnol Biochem. 2005;69:2431–4.
54. Thakur V, Gonzalez MA, Parada M, Martinez RD, Chattopadhyay M. Role of histone deacetylase inhibitor in diabetic painful neuropathy. Mol Neurobiol. 2024;61:2283–96.
55. Tong M, Jun T, Nie Y, Hao J, Fan D. The role of the Slit/Robo signaling pathway. J Cancer. 2019;10:2694–705.
56. Treede R-D, Jensen TS, Campbell JN, Cruccu G, Dostrovsky JO, Griffin JW, et al. Neuropathic pain: redefinition and a grading system for clinical and research purposes. Neurology. 2008;70:1630–5.
57. Wang L, Luo T, Bao Z, Li Y, Bu W. Intrathecal circHIPK3 shRNA alleviates neuropathic pain in diabetic rats. Biochem Biophys Res Commun. 2018;505:644–50.
58. Wang Y, Karlsson R, Jylhävä J, Hedman ÅK, Almqvist C, Karlsson IK, et al. Comprehensive longitudinal study of epigenetic mutations in aging. Clin Epigenetics. 2019;11:187.
59. Wormuth C, Lundt A, Henseler C, Müller R, Broich K, Papazoglou A, et al. Review: Cav2.3 R-type Voltage-Gated Ca2+ Channels - Functional Implications in Convulsive and Non-convulsive Seizure Activity. TONEUJ. 2016;10:99–126.
60. Xiao Y, Theile JW, Zybura A, Pan Y, Lin Z, Cummins TR. A-type FHFs mediate resurgent currents through TTX-resistant voltage-gated sodium channels. Elife. 2022;11:e77558.
61. Yu W, Zhao G-Q, Cao R-J, Zhu Z-H, Li K. LncRNA NONRATT021972 was associated with neuropathic pain scoring in patients with type 2 diabetes. Behav Neurol. 2017;2017:2941297.
62. Yuan B-T, Li M-N, Zhu L-P, Xu M-L, Gu J, Gao Y-J, et al. TFAP2A is involved in neuropathic pain by regulating Grin1 expression in glial cells of the dorsal root ganglion. Biochem Pharmacol. 2024;227:116427.
63. Zamponi GW, Striessnig J, Koschak A, Dolphin AC. The physiology, pathology, and pharmacology of voltage-gated calcium channels and their future therapeutic potential. Pharmacol Rev. 2015;67:821–70.
64. Zhang F, Gu X, Yi S, Xu H. Dysregulated transcription factor TFAP2A after peripheral nerve injury modulated Schwann cell phenotype. Neurochem Res. 2019;44:2776–85.

65. Zhang H-H, Zhang Y, Wang X, Yang P, Zhang B-Y, Hu S, et al. Circular RNA profile in diabetic peripheral neuropathy: analysis of coexpression networks of circular RNAs and mRNAs. Epigenomics. 2020;12:843–57.

Publisher's Note